Carbochlorination Kinetics of Titanium Dioxide with Carbon and Carbon Monoxide as Reductant

FENGLIN YANG and VLADIMIR HLAVACEK

Kinetic study of the chlorination of titanium dioxide (rutile and anatase) was carried out in a fixed-bed reactor at temperature ranging from 800 °C to 1000 °C and normal pressure. In our experiment, titanium dioxide powder and gaseous chlorine with carbon or carbon monoxide as reductant were used. The products of the reaction are all in gaseous phase under the temperatures and pressure studied. With CO as reductant, reaction is of noncatalytic gas-solid nature and experimental data fit the shrinking core model. When using C as reductant, solid-solid reaction is involved. Reactivity is highly enhanced by solid carbon and it is concluded that an activated C-TiO_2-Cl complex contributes to the enhanced reactivity. A reaction model based on phase boundary control applies to the experimental data. Thermodynamic analysis supports the experimental observation.

I. INTRODUCTION

IT is well known that natural reserves of certain ores are limited and become gradually depleted. Alternative sources may be low-grade minerals or industrial wastes. For extraction of oxides of transition group metals, a chlorination process can be used. It provides good yield and purity in metal recovery at reasonable cost and, therefore, is being used more frequently in the field of metal extraction from ores and minerals.

Most transition group metals exist in ores and minerals in the form of metal oxides. Carbochlorination of the metal oxides can be achieved by using a chlorinating agent (*e.g.*, Cl_2, HCl, CCl_4, $COCl_2$, *etc.*) and a reductant (*e.g.*, CO, C) as oxygen sink. For example, when using Cl_2 and CO, the following general reaction applies:

$$M_aO_b + bCO + bCl_2 = aMCl_{(2b/a)} + bCO_2$$

Here, M represents the transition group metal in question.

The volatile chlorides of transition metals can be condensed from the effluent gas stream and separated by distillation or sublimation to high-purity products.

There is a voluminous literature on carbochlorination. Articles and patents have been published concerning the chlorination of alumina,[1–4] silicon dioxide,[5] Nb_2O_5,[6] coal flyash,[7] MoO_3,[8,9] V_2O_5,[10] and other minerals like bauxite[11,12] and iron-bearing titaniferous materials.[13,14,15] Investigations of kinetic aspects and the effect of some factors on the recovery of a given metal were covered.

Brain and Schuler[16] studied the chlorination of pure titanium dioxide by putting tablets of TiO_2 and carbon side by side into a reactor. They concluded that the chlorination rate of TiO_2 was 40 to 50 times faster with TiO_2-C contact than in the absence of carbon and the acceleration of the chlorination rate decreases with increasing TiO_2-C separation. Dunn[17] carried out the chlorination of TiO_2 bearing minerals (ilmenite) using CO + Cl_2 or $COCl_2$ as chlorinating agent and reductant. He claimed that the effect of concentration of both CO and Cl_2 to the reaction rate is linear and that phosgene tends to decompose at high temperatures and approach the CO + Cl_2 behavior. Youn and Park[18] and Zhou and Sohn[19] developed mathematical modeling of fluidized-bed chlorination of rutile. However, systematic investigation of kinetic data of carbochlorination of titanium dioxide is not readily available in the literature.

In our study, chlorination of two kinds of oxides, TiO_2(R)(rutile, powder, <5 μm, 99.9 pct) and TiO_2(A) (anatase, powder, -325 mesh, 99 pct), was carried out. Temperatures of 800 °C and 1000 °C were chosen as reaction temperatures. The total pressure of 102.1 kPa inside the reactor was kept. The combinations of chlorine with solid carbon or chlorine with carbon monoxide were used for chlorination.

The major objective of this study is to understand better the carbochlorination process of TiO_2 by analyzing the intrinsic kinetics and the effect of other factors on the process and to provide rate expression and other kinetic data for design and scale-up purposes.

II. THERMODYNAMIC ANALYSIS

Chemical equilibrium calculations of chlorination of TiO_2 with either carbon or CO as reductant were performed. The NASA–Lewis Research Center's computer program[20] was employed for chemical equilibrium calculations. This program is based on the minimization of free energy. Chemical equilibrium compositions of the reaction systems at normal pressure and different temperatures were obtained.

A. *CO as Reductant*

Thermodynamic calculations are reported in Figures 1 (a) through (c). Figure 1(a) gives the initial stoichiometric ratio of reactants: from 200 °C to 1000 °C, compositions of products are stable and conversion of TiO_2 is complete. For temperatures higher than 1000 °C, a small fraction of TiO_2 remains unreacted.

Figures 1(b) and (c) give the initial ratio of reactants with excess of CO and Cl_2: these two cases resemble the real carbochlorination process in which a sufficient amount of

FENGLIN YANG, Research Assistant, and VLADIMIR HLAVACEK, Professor, are with the Department of Chemical Engineering, SUNY at Buffalo, Buffalo, NY 14260.

Manuscript submitted January 15, 1998.

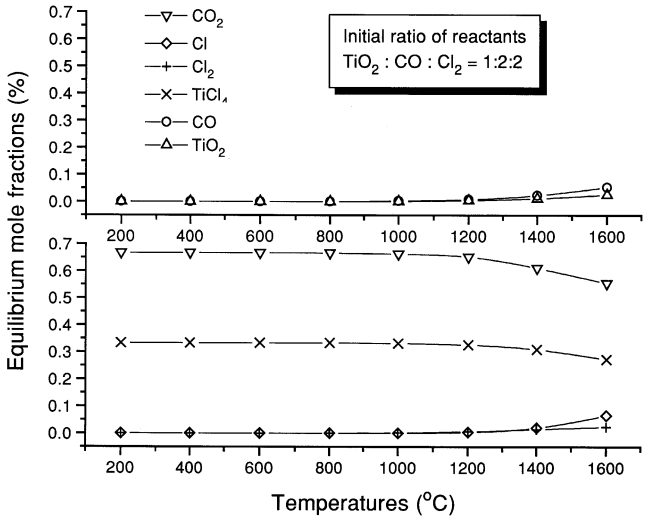

(*a*)

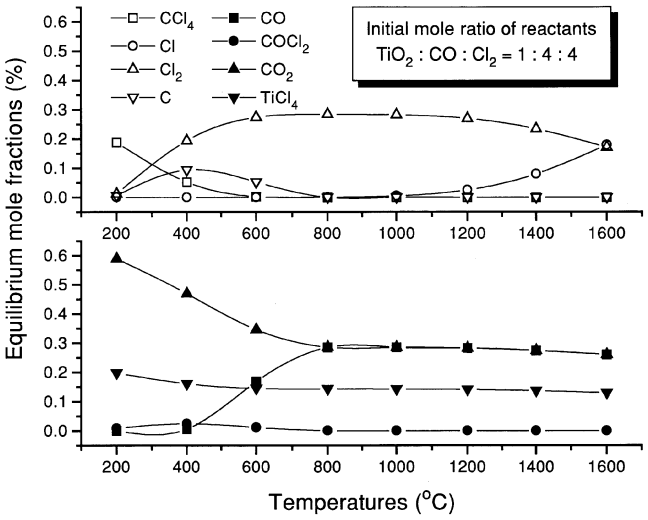

(*b*)

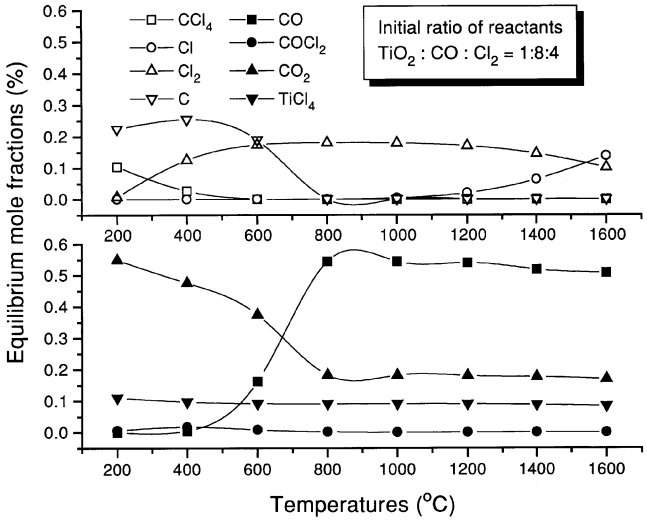

(*c*)

Fig. 1—Chemical equilibrium composition for $TiO_2 + Cl_2 + CO$ reaction system: (*a*) TiO_2:CO:Cl_2 = 1:2:2, (*b*) TiO_2:CO:Cl_2 = 1:4:4, and (*c*) TiO_2:CO:Cl_2 = 1:8:4.

reactant gases flow through the bed of solid reactant particles. Conversion is complete in the temperature domain considered. Thermodynamic analysis reveals that CCl_4 exists in the system as a product, which is not desired. It disappears at temperatures higher than 800 °C. By comparison of the result in Figure 1(b) with that in Figure 1(c), it is seen that the increased CO/Cl_2 ratio has no effect on the product compositions.

B. *Carbon as Reductant*

Results of thermodynamic calculations are given in Figures 2 (a) through (c). In Figure 2(a), the initial ratio of reactants is stoichiometric: conversion of TiO_2 is complete at all temperatures considered. Titanium tetrachloride, $TiCl_4$, is stable up to 1200 °C. With higher temperatures, decomposition to $TiCl_3$ begins. CO_2 alone is generated as a product other than titanium chlorides at temperatures below 400 °C, but CO appears above 900 °C.

Figures 2(b) and (c) give the initial ratio of reactants with excess of C and Cl_2: this situation represents the real process in which carbon is in excess in the solid phase and a sufficient amount of chlorine passes through the solid bed. Titanium dioxide, TiO_2, is completely converted in the temperature region considered. The equilibrium products are $TiCl_4$, CCl_4, $COCl_2$, CO, and CO_2. At temperatures above 800 °C, $TiCl_4$ and CO are the only two stable products. Thermodynamic analysis indicates that the increased ratio of carbon to TiO_2 has an insignificant effect on the product compositions.

III. EXPERIMENTAL SETUP AND PROCEDURE

A. *Reactor System*

The reactor consisted of a quartz tube (o.d. 32.5 mm, wall thickness 2.5 mm, and length 610 mm) that was placed in a Lindberg tube furnace (1100 °C TF 55030 A) equipped with a temperature controller. The reacting sample was held in a ceramic boat (length 50 mm, width 12 mm, and depth 9 mm) that was located inside the reactor tube. Chlorine, carbon monoxide, and argon stored in the cylinders were used as gases. Mass flowmeters and metering valves were used to control the flow rate. Two-stage scrubbers with 5 pct caustic soda solution neutralized the exit gas.

Temperature inside the reactor tube was determined in-

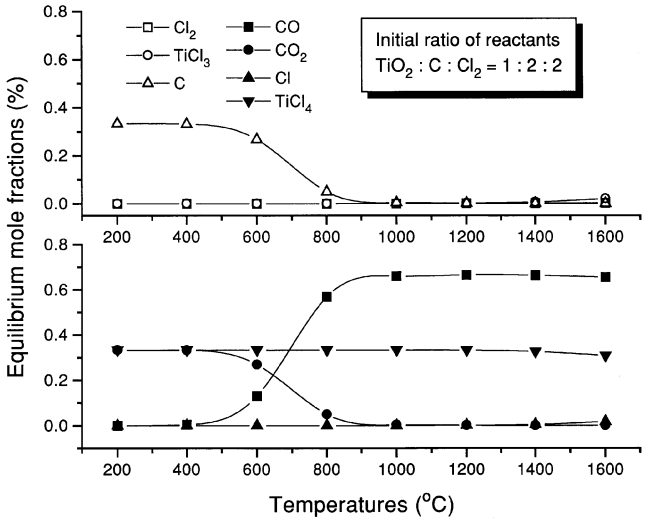

(*a*)

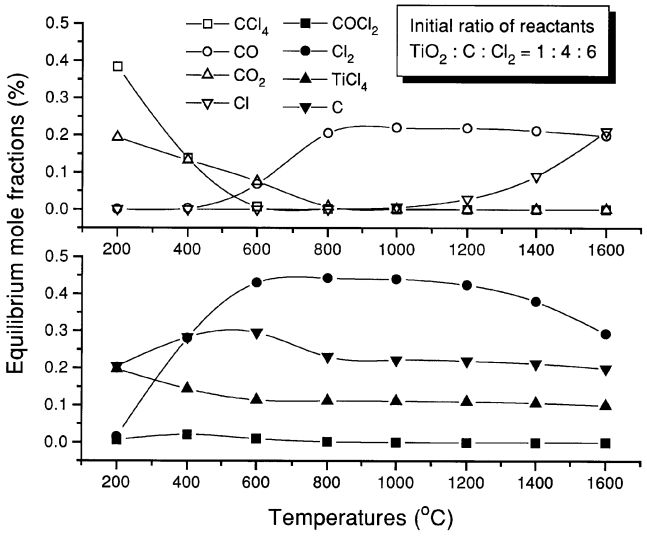

(*b*)

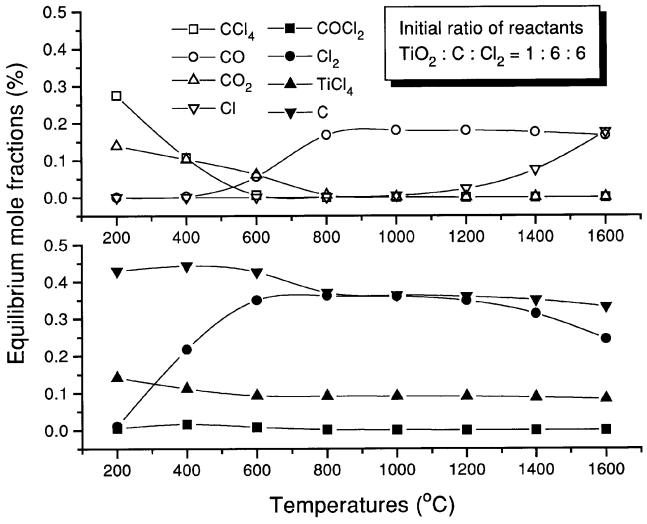

(*c*)

Fig. 2—Chemical equilibrium composition for $TiO_2 + Cl_2 + C$ reaction system: (*a*) TiO_2:C:Cl_2 = 1:2:2, (*b*) TiO_2:C:Cl_2 = 1:4:6, and (*c*) TiO_2:C:Cl_2 = 1:6:6.

directly through calibration by measuring the local axial temperature profile inside the tube under blank run, *i.e.*, with inert gas.

B. *Supporting Equipment*

An analytical balance (Model 200 analytical balance, Sartorius Corporation, Long Island, NY) was used for the measurement of the sample mass before and after the experiment. The balance has a maximum sensitivity of 0.0001 g. Mixing of oxide and carbon powder was conducted by using a Turbula Shaker-Mixer (Type T2C, Impandex Inc., Maywood, NJ). *A* thermogravimetric analyzer (TGA) (Model ST-736, temperature ranging from 20 °C to 1600 °C, maximum sensitivity of 0.0001 g, Harrop Industries, Columbus, OH) was used to determine the contents of unreacted oxide and carbon in the chlorinated sample.

Particle size and morphologies were characterized by three measurements: scanning electron microscope (SEM) (Model S-800, Hitachi, Gaithersburg, MD), sedimentation particle size analysis (Model CAPA-700, Horiba Instruments Inc., Irvine, CA), and BET surface area (Model ASAP2000, Micromeritics Instrument Corporation, Norcross, GA).

C. *Procedure*

Samples chlorinated were either pure oxide or oxide premixed with carbon powder. Argon was selected as purging gas before and after chlorination.

The ceramic boat containing a known amount of sample was slowly inserted in the middle of the reactor, the reactor was sealed, and argon was introduced at a flow rate of 200 mL/min to purge the system. Reaction temperature (either 800 °C or 1000 °C) was set and the furnace was switched on. The heating rate was 50 °C/min. Ten minutes after the temperature reached the set point, the argon flow was shut off and gaseous reactants (Cl_2 or Cl_2/CO) were fed into the reactor at the desired flow rate. After specified chlorination time, Cl_2 or Cl_2/CO was replaced by argon again to purge the system. The reaction temperature was kept for 5 more minutes in an argon stream to ensure a complete removal of the volatile chloride produced. Afterward, power was switched off and the furnace body was opened for quick

Table I. Conversion *vs* Gas Flow Rate for TiO_2 + Cl_2 + CO

Inlet Gas Flow Rate (mL/min)	Conversion of TiO_2(R) (Pct)	Conversion of TiO_2(A) (Pct)
111.50	19.21	18.92
221.15	26.44	20.40
413.25	33.11	26.74
500.00	32.71	28.61
600.00	32.90	28.70

cooling. After the reactor tube was cooled to room temperature, purging was discontinued and the sample was taken out. Both the sample and the ceramic boat were weighted. For samples of oxide mixed with carbon, TGA analysis was conducted to get the conversion of oxides.

IV. MODELING AND DATA FITTING

A. *Using CO as Reductant*

1. *Reaction model*

Under the reaction temperatures and pressure used, this system is of a gas-solid type. TiO_2 is the only solid phase. The nonporous solid TiO_2 particle (that was proved by SEM micrographs shown in Figures 7(a) and (b)) undergoes a reaction of the type

$$TiO_2\ (\text{solid}) + 2Cl_2\ (\text{gas}) + 2CO\ (\text{gas}) \rightarrow TiCl_4\ (\text{gas}) + 2CO_2\ (\text{gas}) \quad [1]$$

Since the products are in gaseous state and no ash is formed on the surface of the solid particles during reaction, the reacting particle shrinks as the reaction is going on, and finally disappears.

The reaction can be summarized by the following three steps.[21]

Step 1. Diffusion of gaseous reactants, Cl_2 and CO, from the bulk of the gas stream through the gas film to the surface of the TiO_2 solid particle. It should be emphasized that each individual particle is nonporous.

Step 2. Reaction of gaseous reactants (Cl_2 and CO) with the solid TiO_2 particle on the solid surface.

Step 3. Diffusion of reaction products, $TiCl_4$ and CO_2, from the surface of the solid through the gas film back into the bulk of the gas stream.

To determine the intrinsic kinetics, the reaction conditions were chosen such that the mass transfer (steps 1 and 3) did not control the overall reaction rate. This entailed working with sufficiently small sample size and high gaseous flow rate. Sample size of 1.5 g was used. This sample size guaranteed low bed depth and meanwhile was large enough to keep the mass measurement error under control. Argon was used as a diluting gas to adjust the particular value of gaseous precursors.

The flow rate necessary to eliminate mass transfer resistance was determined experimentally. Experiments were done at 1000 °C with $P_{\text{total}} = 102.1$ kPa, $p_{Cl_2} = 37.6$ kPa, and $p_{CO} = 64.5$ Pa under different flow rates. Reaction time was 10 minutes. The dependence of conversion on the gas flow rate is shown in Table I. It is obvious from these results that conversion of either TiO_2(R) or TiO_2(A) does not change with the increase of flow rate above 500 mL/min. Therefore, the experiments were performed at this flow rate.

Mass transfer limitations (steps 1 and 3) were eliminated in this study, and therefore, chemical reaction became the only rate-limiting step (step 2). In this case, the model of shrinking unreacted solid particle with chemical reaction as the controlling step was considered.

We will assume irreversible reaction and spherical geometry of the TiO_2 particle. Based on the unit surface of the shrinking particle, the rate of reaction,

$$TiO_2\ (s) + 2Cl_2\ (g) + 2CO\ (g) \rightarrow TiCl_4\ (g) + 2CO_2\ (g) \quad [2]$$

can be expressed as follows:[21]

$$-\frac{2}{4\pi r^2}\frac{dN_{TiO_2}}{dt} = -\frac{1}{4\pi r^2}\frac{dN_{CL_2}}{dt} = -\frac{1}{4\pi r^2}\frac{dN_{CO}}{dt} = k_s p_{Cl_2}^m\, p_{CO}^n \quad [3]$$

Here, k_s is the rate constant for the surface reaction and r is a radius of the shrinking particle.

Writing N_{TiO2} in terms of the shrinking radius, we have

$$-dN_{TiO_2} = -\frac{1}{2}dN_{Cl_2} = -\frac{1}{2}dN_{CO} = -\rho_{TiO_2}\,dV = -\rho_{TiO_2}\,d\left(\frac{4}{3}\pi r^3\right) = -4\pi\rho_{TiO_2}\,r^2 dr \quad [4]$$

Substitution of Eq. [4] into Eq. [3] gives the rate in terms of the shrinking radius of the unreacted core:

$$-2\rho_{TiO_2}\frac{dr}{dt} = k_s p_{Cl_2}^m p_{CO}^n \quad [5]$$

After integration of Eq. [5], we have

$$-2\rho_{TiO_2}\int_{r_0}^{r} dr = k_s p_{Cl_2}^m p_{CO}^n \int_0^t dt \quad [6]$$

$$t = \frac{2\rho_{TiO_2}}{k_s p_{Cl_2}^m p_{CO}^n}(r_0 - r) \quad [7]$$

The time τ necessary for completing the conversion of the particle can be calculated when $r = 0$; *i.e.*,

$$\tau = \frac{2\rho_{TiO_2} r_0}{k_s p_{Cl_2}^m p_{CO}^n} \quad [8]$$

Combining Eqs. [7] and [8] and also noting that

$$1 - X_{TiO_2} = \frac{V_{\text{unreacted}}}{V_{\text{total}}} = \frac{\frac{4}{3}\pi r^3}{\frac{4}{3}\pi r_0^3} = \left(\frac{r}{r_0}\right)^3$$

We can get the following correlation between the reaction time and the shrinking radius (or conversion of the particle) in terms of τ:

$$\frac{t}{\tau} = 1 - \frac{r}{r_0} = 1 - (1 - X_{TiO_2})^{1/3} \quad [9]$$

Here, X_{TiO2} is the conversion of TiO_2.

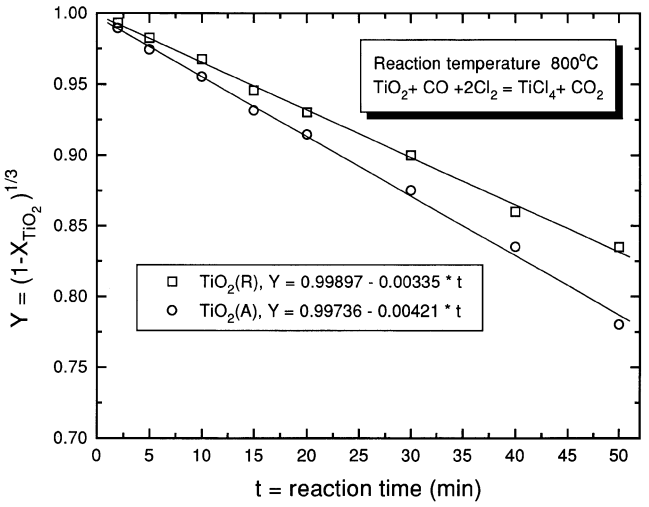

Fig. 3—TiO_2 conversion *vs* time at 800 °C by Cl_2 + CO.

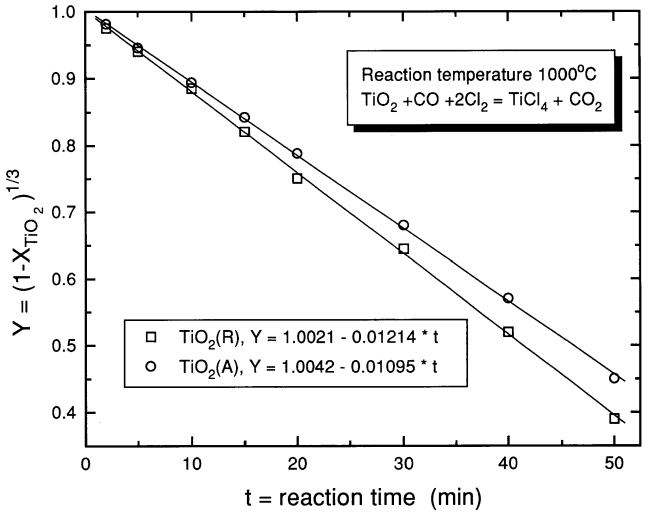

Fig. 4—TiO_2 conversion *vs* time at 1000 °C by Cl_2 + CO.

2. *Fitting experimental data to model*

Equation [9] can be expressed in the following form:

$$(1 - X_{TiO_2})^{1/3} = 1 - \frac{t}{\tau} \qquad [10]$$

The plot of $(1 - X_{TiO_2})^{1/3}$ *vs* t should yield a straight line with slope of $-\frac{1}{\tau}$.

Conversion *vs* time relation was obtained experimentally at 800 °C and 1000 °C with flow rate = 500 mL/min, P_{total} = 102.1 kPa, PCl_3 = 37.6 kPa, and p_{CO} = 64.5 kPa. Results are shown in Figures 3 and 4. The slopes and the corresponding values of τ are as follows.

$$\text{At 1000 °C: for TiO2(R), } -\frac{1}{\tau_{1000\ °C}} = -0.01214 \quad \tau_{1000\ °C} = 82.4 \text{ min}$$

$$\text{for TiO2(A), } -\frac{1}{\tau_{1000\ °C}} = -0.01095 \quad \tau_{1000\ °C} = 91.3 \text{ min}$$

$$\text{At 800 °C: for TiO2(R), } -\frac{1}{\tau_{800\ °C}} = -0.00335 \quad \tau_{800\ °C} = 298.5 \text{ min}$$

$$\text{for TiO2(A), } -\frac{1}{\tau_{800\ °C}} = -0.00421 \quad \tau_{800\ °C} = 237.5 \text{ min}$$

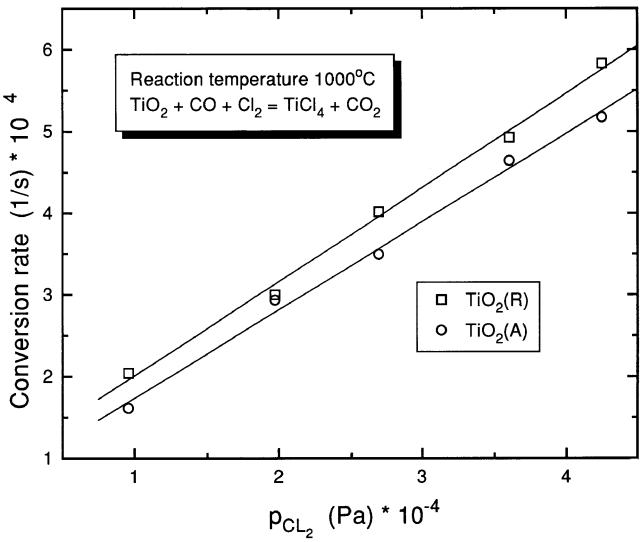

Fig. 5—Chlorine partial pressure *vs* TiO_2 conversion rate with CO as reductant.

Rate constant k_s can be calculated from Eq. [8] once the reaction order and other physical properties such as particle size and density of the solid are known.

3. *Determination of reaction order*

Rate of reaction has the following form:

$$r = k_s p_{Cl_2}^m p_{CO}^n \qquad [11]$$

In order to get reaction order, experiments were conducted in two stages.

(1) Reaction order with respect to Cl_2, m

Reactions were carried out at constant P_{total} (=102.1 kPa) and p_{co} (=23.8 kPa). Conversion data of solid TiO_2, X_{TiO_2}, at different p_{Cl_2} were obtained. Reaction conditions were temperature = 1000 °C, flow rate = 500 mL/min, and reaction time t = 5 min. Argon was used as dilution gas to keep constant flow rate, constant P_{total}, and constant p_{CO} when p_{Cl_2} was decreased. Under the preceding conditions, Eq. [11] could be written in the form

$$r = k_s' p_{Cl_2}^m \qquad [12]$$

where

$$k_s' = k_s p_{CO}^n$$

Experimental data shown in Figure 5 indicate that the plot of p_{Cl_2} *vs* conversion rate ($\Delta X_{TiO_2}/\Delta t$) is a straight line. It can be concluded therefore that the chlorination of both TiO_2(R) and TiO_2(A) is of first order, m = 1.

(2) Reaction order with respect to CO, n

Reaction conditions were similar to those in stage (1); the only difference was that p_{Cl_2} = 23.8 kPa remained constant instead of p_{CO}.

The logarithmic form of Eq. [11] is

$$\ln r = n \ln p_{CO} + \ln (k_s p_{Cl_2}) \qquad [13]$$

The plot of ln p_{CO} *vs* ln ($\Delta X_{TiO_2}/\Delta t$), Figure 6, gives rise to a straight line. The slopes are

n = 0.8659 for TiO_2(R)

n = 0.8968 for TiO_2(A).

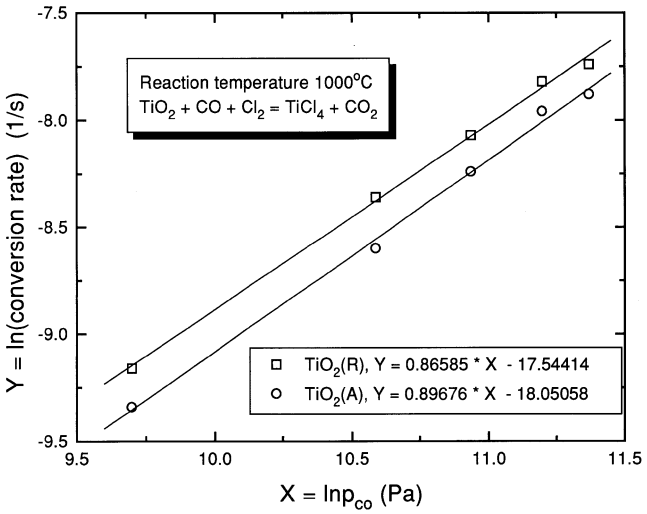

Fig. 6—CO partial pressure *vs* TiO_2 conversion rate.

4. *Particle size and density of solid TiO_2*

The densities of $\rho^{\text{mass}}_{\text{TiO2(R)}} = 4.23$ g/cm³ and $\rho^{\text{mass}}_{\text{TiO2(A)}} = 3.90$ g/cm³ are provided by the manufacturer. The corresponding molar densities are $\rho_{\text{TiO2(R)}} = 0.05294$ mole/cm³ and $\rho_{\text{TiO2(A)}} = 0.04881$ mole/cm³.

The radius of the particles can be determined in three ways.

(1) SEM photographs: from Figures 7(a) and (b), the radii of the particles (after preheating and before chlorination) were in the range of about 0.18 to 0.50 μm for TiO_2(R) and 0.07 to 0.18 μm for TiO_2(A).
(2) Sedimentation particle size analysis: the measured average sedimentation particle size radii (R_S) for TiO_2(R) and TiO_2(A) were 0.35 and 0.14 μm, respectively.
(3) BET surface area: multipoint (five points) measurement of the oxides before chlorination gave the BET surface areas of 2.8533 m²/g for TiO_2(R) and 9.7710 m²/g for TiO_2(A). Assuming single effective particle size and spherical geometry, the effective radius (R_e) can be expressed by the following relation:

$$R_e = \frac{3}{\rho^{\text{mass}}_{\text{TiO2}}\text{BET}} \qquad [14]$$

The effective particle radii (R_e) obtained from Eq. [14] are 0.249 μm for TiO_2(R) and 0.0787 μm for TiO_2(A).

It is obvious from the micrographs shown in Figures 7(a) and (b) that the particles are somewhat irregular for both types of oxides. In addition, there is a distribution of particle sizes. It is important to choose a correct average particle size in order to quantify the reactivity of the powder with sufficient accuracy. Since the photographs were taken by picking up the sample area randomly, the radius obtained may or may not reflect the real particle size distribution. Therefore, those data can be taken as reference rather than being used to describe the reactivity. Due to the irregularities of the power particles, it is unsatisfactory to use the sedimentation particle size as a measure of such an average particle size. On the contrary, the reactivity should depend on the total surface area that is exposed to the environment. Therefore, a much better approximation than simply using the sedimentation particle size is to assume some idealized geometry (sphere in this study) and then to use the actual measured surface area to calculate an effective particle size, R_e.[22] This approach also conforms to the suggestions of Szekely *et al.*[23]

5. *Rate constant and other kinetic data*

The reaction rate can be written as

$$r = k_s p_{\text{Cl}_2} p_{\text{CO}}^{0.8659} \qquad \text{for } TiO_2\text{(R)} \qquad [15]$$

$$r = k_s p_{\text{Cl}_2} p_{\text{CO}}^{0.8968} \qquad \text{for } TiO_2\text{(A)} \qquad [16]$$

$$k_s = k_s^o \exp\left(-\frac{Ea}{RT}\right) \qquad [17]$$

By substituting the known data of $\tau_{800°C}$, $\tau_{1000°C}$, ρ_{TiO_2}, $r_o(=R_e)$, $p^m_{Cl_2}$, and p^n_{CO} into Eq. [8], the rate constants $k_{S,1000°C}$ and $k_{S,800°C}$ can be calculated. Activation energies and frequency factor k_s^o can be determined from Eq. [17].

The calculation is summarized in Table II.

B. *Carbon as Reductant*

1. *Reaction system*

When using carbon as reductant at temperatures of 800 °C and 1000 °C, the possible reactions are the following:

$$TiO_2\ (s) + C\ (s) + 2Cl_2\ (g) \rightarrow TiCl_4\ (g) + CO_2\ (g) \qquad [18]$$

$$TiO_2\ (s) + 2C\ (s) + 2Cl_2\ (g) \rightarrow TiCl_4\ (g) + 2CO\ (g) \qquad [19]$$

$$TiO_2\ (s) + 2CO\ (g) + 2Cl_2\ (g) \rightarrow TiCl_4\ (g) + 2CO_2\ (g) \qquad [20]$$

Equations [18] and [19] should be considered because of the following arguments.

(1) Equation [20] is exactly the same as Eq. [1] or [2]. Kinetic data from Section A and from this section indicate that the reaction rate with CO as reductant (Eq. [20]) is much slower than that with carbon as reductant (Eqs. [18] and [19]).
(2) Thermodynamic analysis of this system reveals that the ratio of CO/CO_2 at equilibrium is 40 for reaction at 800 °C and 620 for reaction at 1000 °C. That illustrates that Eq. [19] is dominant.
(3) At the high flow rate we used, CO is removed from the surface of the particles by the incoming reactant gases as long as it is generated. That makes Eq. [20] unfavorable.

Therefore, this is a solid-solid reaction system in which two solid reactants (TiO_2 and carbon) and one gaseous reactant (chlorine) are involved. The products are gaseous at the reaction temperatures used.

2. *Effect of gas flow rate*

Experiments were made for TiO_2:C = 3:1 (by weight) and Ar:Cl_2 = 2:1 (by volume) at 1000 °C under different total flow rates. Reaction time was 5 minutes. The results are shown in Table III.

It can be inferred from Table III that the mass transfer resistance from gaseous to solid reactants is negligible at flow rates greater than 500 mL/min.

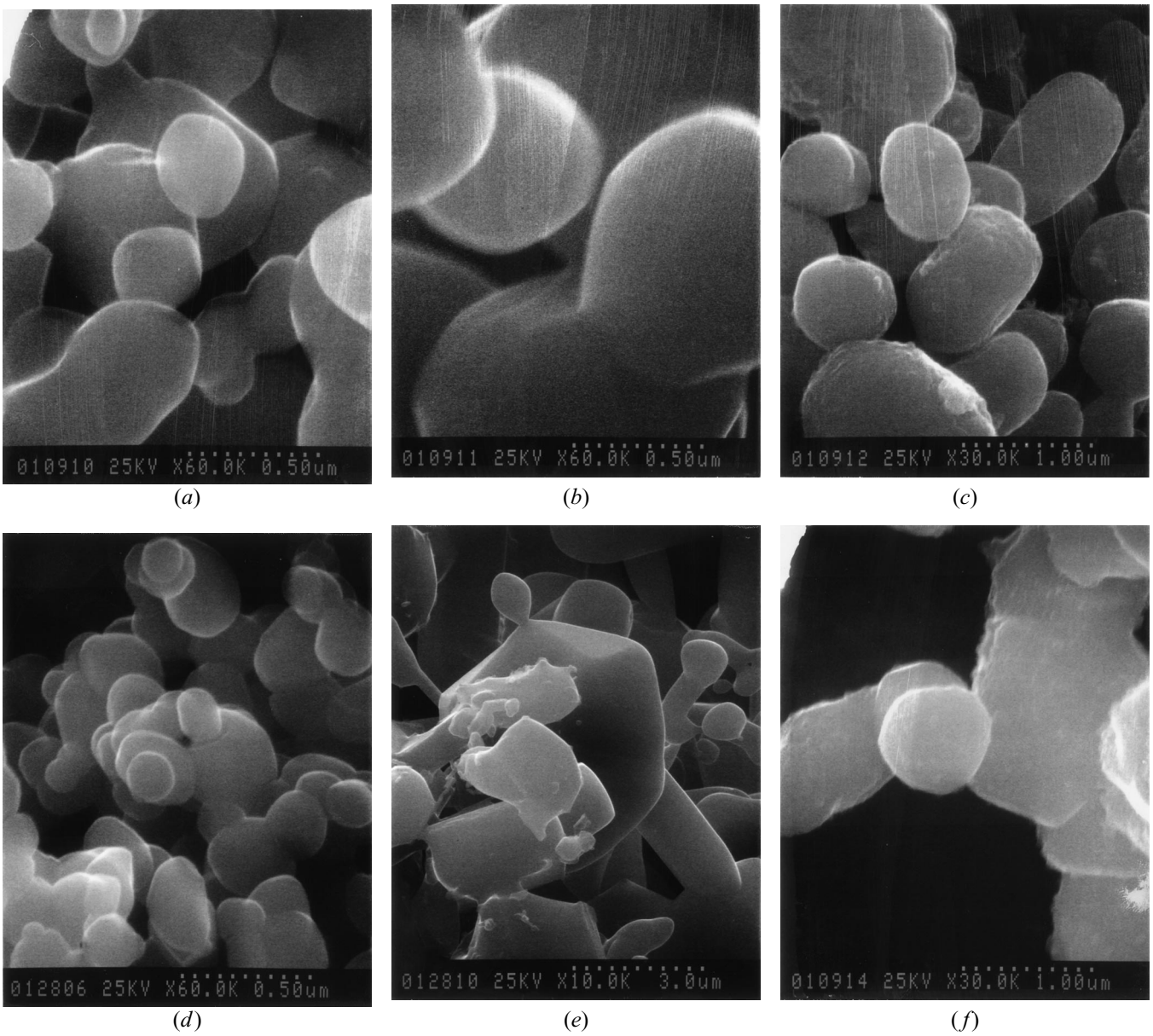

(*a*) (*b*) (*c*)

(*d*) (*e*) (*f*)

Fig. 7—SEM photos: (*a*) TiO_2(R) untreated, (*b*) TiO_2(R) 1000 °C chlorinated by Cl_2 + CO, (*c*) TiO_2(R) 1000 °C chlorinated by Cl_2 + C, (*d*) TiO_2(A) untreated, (*e*) TiO_2(A) 1000 °C chlorinated by Cl_2 + CO, and (*f*) TiO_2(A) 1000 °C chlorinated by Cl_2 + C.

3. *Effect of carbon content*

Chlorination of TiO_2 with different amounts of carbon was performed. Reaction conditions were temperature = 1000 °C, flow rate = 537 mL/min, Ar:Cl_2 = 2:1, reaction time = 5 min. The three weight ratios of TiO_2/carbon tested were TiO_2:C = 3:1, 2:1, and 1:1. All three ratios have carbon in excess according to stoichiometry since the stoichiometric ratio of TiO_2 to carbon should be somewhere between 3.3:1 (based on reaction in Eq. [19]) and 6.6:1 (based on reaction in Eq. [18]).

The results are listed in Table IV. It is evident that the reactivity increased with the increased carbon content. The reason for this is a better contact of TiO_2 and carbon. Reaction rate increased due to the increase of the contacted surface area of these two solid reactants. Another observation is that the ratio of reacted oxide to reacted carbon was changing with different initial ratios. It means that the balance between Eqs. [18] and [19] depends on the carbon content in the system.

4. *Effect of chlorine partial pressure*

Chlorination of samples with TiO_2:C = 1:1 (by weight) at different Cl_2 partial pressures was carried out. Reaction conditions were flow rate = 537 mL/min, temperature = 1000 °C, P_{total} = 102.1 kPa, and reaction time = 5 minutes. Argon was used to adjust the Cl_2 partial pressure and to keep the overall flow rate. A plot of specific reaction rate *vs* Cl_2 partial pressure is shown in Figure 8. It is obvious that the relationship between reaction rate and chlorine partial pressure is linear.

5. *Reaction mechanism and reaction model*

Numerous studies on solid-solid reactions have been reported. Tamhankar and Doraiswamy[24] summarized various aspects of these studies in their review. For mixed powder

Table II. Summary of Calculations of Kinetic Data for $TiO_2 + Cl_2 + CO$ Reaction System

Symbols	Descriptions	Unit	Data of TiO_2(R)	Data of TiO_2(A)
BET	surface area of oxides	cm^2/g	28,533	97,710
R_e $(=r_0)$	effective (initial) particle radius of TiO_2 from BET	cm	2.49×10^{-5}	7.87×10^{-6}
ρ_{TiO_2}	molar density of solid TiO_2	$mole/cm^3$	0.05294	0.04881
m	reaction order w.r.t. Cl_2	—	1	1
n	reaction order w.r.t. CO	—	0.8659	0.8968
p_{Cl_2}	partial pressure of Cl_2	Pa	37,595	37,595
p_{CO}	partial pressure of CO	Pa	64,505	64,505
$\tau_{1000\,°C}$	time required for complete conversion at 1000 °C	min	82.37	91.32
$\tau_{800\,°C}$	time required for complete conversion at 800 °C	min	298.51	237.53
$k_{S,1000\,°C}$	rate constant at 1000 °C	$\frac{mole}{cm^2 \cdot min \cdot (P_a)^{n+1}}$	5.83×10^{-17}	1.09×10^{-17}
$k_{S,800°C}$	rate constant at 800 °C	$\frac{mole}{cm^2 \cdot min \cdot (P_a)^{n+1}}$	1.60×10^{-17}	4.18×10^{-18}
k_s^0	frequency factor	$\frac{g}{cm^2 \cdot min \cdot (P_a)^{n+1}}$	6.01×10^{-14}	1.86×10^{-15}
E_a	activation energy	J/mol	7.34×10^4	5.44×10^4

Table III. Conversion *vs* Gas Flow Rate for $TiO_2 + Cl_2 + C$

Inlet Gas Flow Rate (mL/min)	Conversion of TiO_2(R) (Pct)	Conversion of TiO_2(A) (Pct)
300	18.24	38.96
405	23.07	41.10
500	23.13	41.12
600	23.14	41.12

reactions, the following reaction mechanisms were presented.

Type 1: Product layer diffusion control: a continuous product layer is formed during the initial stages of the reaction, and further reaction takes place by bulk diffusion of mobile reactant species through this product layer, which is the rate-controlling step.

Type 2: Phase boundary reaction control: when the diffusion of the reactant species through the product layer is fast compared to reaction, the kinetics is controlled by phase boundary reactions.

Type 3: Nuclei growth control: two steps are considered—formation of the nuclei of the product phase at active sites and the growth of these nuclei.

In our reaction system, the products are all in gaseous phase. TiO_2 particle is shrinking and no solid product layer exists. These facts are in agreement with thermodynamic analysis and the results from SEM analysis. Direct surface contact between two solid reactants remains until one solid reactant disappears. In this case, solid-solid diffusion through product layer should not be the controlling step. *Type 1* does not apply. Also, *Type 3* is not relevant to our system.

Result from our experiments showed that at temperatures from 800 °C to 1000 °C, reaction between any two of the three reactants (TiO_2, carbon, and chlorine) does not take place or takes place with extremely low conversion. Thermodynamic calculations verify this observation. Based on these results and also from the fact that the reaction rate depends on both chlorine partial pressure and carbon content, it is reasonable to assume that at high temperature, in the process of reaction, an activated C-TiO_2-Cl complex is formed on the TiO_2/C/Cl_2 interface; this active complex is then decomposed into CO and $TiCl_4$. The rate of formation of this active complex should be proportional to the surface area of TiO_2 particle and is the controlling step. This mechanism falls into *Type 2* mentioned previously. Once this complex is formed, it decomposes immediately. Therefore, the concentration of the complex is very low.

Based on the preceding analysis, consider a sphere of nonporous TiO_2 of initial radius r_o and density ρ^{mass} and suppose the rate of chlorination is proportional to the receding surface area, A, of the remaining TiO_2 particle. If M is the mass of the remaining oxide particle, a rate equation can be derived as follows:

$$-\frac{dM}{dt} = kA \qquad [21]$$

where k is a proportional constant and is a function of temperature, carbon content, and chlorine partial pressure.

$$A = 4\pi r^2 \qquad [22]$$

$$M = \rho^{mass} \cdot \frac{4}{3}\pi r^3 \qquad [23]$$

If we differentiate Eq. [23] with respect to time, we obtain

$$\frac{dM}{dt} = 4\rho^{mass}\,\pi r^2 \frac{dr}{dt} \qquad [24]$$

If we substitute Eqs. [22] and [24] into Eq. [21] and then integrate, we obtain

$$-\rho^{mass}\int_{r_0}^{r} dr = k\int_0^t dt \qquad [25]$$

From Eq. [25],

$$r_0 - r = \frac{k}{\rho^{mass}}\,t \qquad [26]$$

Also,

Table IV. Effect of Carbon Content on Conversion for $TiO_2 + Cl_2 + C$ Reaction System

TiO_2:C (Weight Ratio)	Conversion of TiO_2(R) (Pct)	TiO_2(R) (Reacted) / C (Reacted)	Conversion of TiO_2(A) (Pct)	TiO_2(A) (Reacted) / C (Reacted)
3:1	23.65	2.06:1	41.08	2.55:1
2:1	26.94	1.85:1	46.86	2.21:1
1:1	35.00	1.71:1	56.45	2.21:1

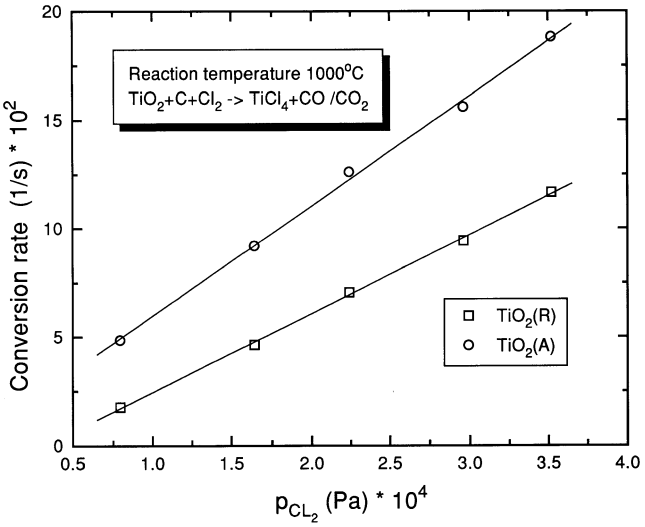

Fig. 8—Chlorine partial pressure *vs* TiO_2 conversion rate with C as reductant.

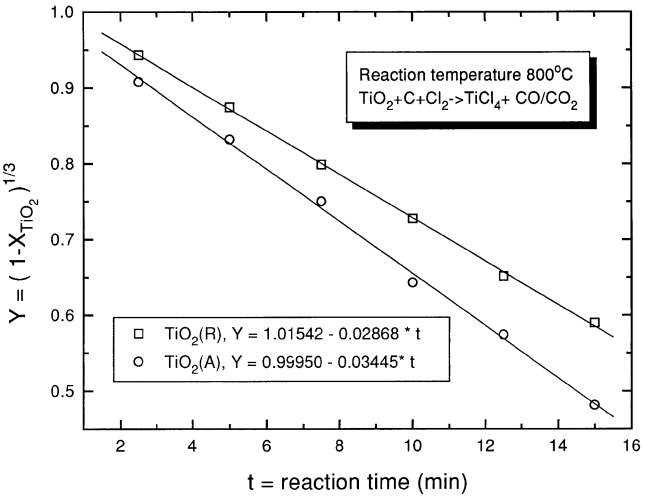

Fig. 9—TiO_2 conversion *vs* time at 800 °C by Cl_2 + C.

$$X_{TiO_2} = \frac{\frac{4}{3}\pi(r_0^3 - r^3)\rho^{mass}}{\frac{4}{3}\pi r_0^3 \rho^{mass}} = \frac{r_0^3 - r^3}{r_0^3} \qquad [27]$$

If we combine Eq. [26] with [27], we obtain

$$1 - (1 - X_{TiO_2})^{1/3} = \frac{k}{r_0\rho^{mass}} t = Kt \qquad [28]$$

This equation has an identical form with the expression previously derived for the gas-solid reaction.

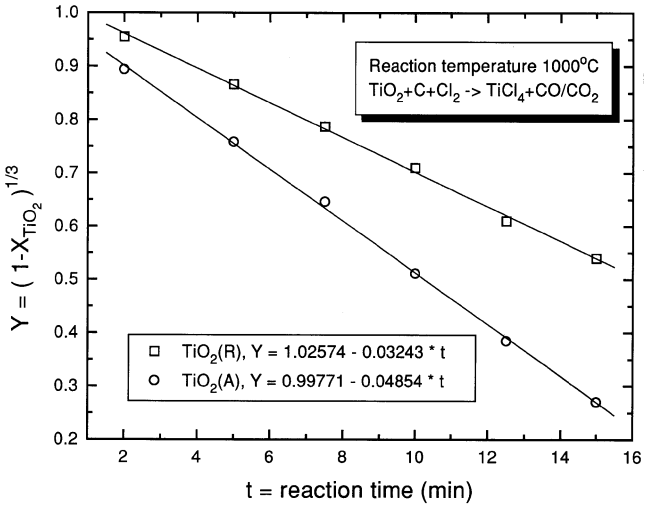

Fig. 10—TiO_2 conversion *vs* time at 1000 °C by Cl_2 + C.

6. *Fitting experimental data to model*

Chlorination of TiO_2:C = 1:1 (by weight) was carried out at 800 °C and 1000 °C. To eliminate mass transfer resistance, a total flow rate of 537 mL/min was chosen and argon was used as the diluting gas. Pressures in the system were P_{total} = 102.1 kPa, p_{Cl_2} = 35.0 kPa, and p_{Ar} = 67.1 kPa. Plots of conversion *vs* time are shown in Figures 9 and 10. The relation of $(1 - X_{TiO_2})^{1/3}$ *vs* time is linear, as expected from Eq. [28]. From the slopes of the plots, the constant K can be obtained and k can be calculated.

As k is a function of temperature, carbon content, and chlorine partial pressure, it can be expressed as

$$k = k_C \cdot k_{Cl_2} \cdot k_T \qquad [29]$$

where k_C, k_{Cl_2}, and k_T represent the effect of carbon content, chlorine partial pressure, and reaction temperature, respectively.

From the linear relationship between reaction rate and chlorine partial pressure in Figure 8, we conclude $k_{Cl_2} = p_{Cl_2}$. We also assume that with sufficient amount of carbon, k_c is constant.

Assuming $k_T = k_T^o \exp\left(-\frac{Ea}{RT}\right)$, Eq. [29] yields

$$k = p_{Cl_2} k_C k_T^0 \exp\left(\frac{-E_a}{RT}\right) \qquad [30]$$

or

$$k = p_{Cl_2} k^0 \exp\left(\frac{-E_a}{RT}\right) \qquad [31]$$

where $k^O = k_C k_T^o$ is the pseudo frequency factor.

From the slopes in Figures 9 and 10, $K_{1000°C}$ and $K_{800°C}$

Table V. Summary of Calculations of Kinetic Data for $TiO_2 + Cl_2 + C$ Reaction System

Symbols	Descriptions	Unit	Data of TiO_2(R)	Data of TiO_2(A)
R_e ($=r_0$)	effective particle radius of TiO_2 from BET	cm	2.49×10^{-5}	7.87×10^{-6}
$\rho_{TiO_2}^{mass}$	density of solid TiO_2	g/cm^3	4.23	3.90
p_{Cl_2}	partial pressure of Cl_2	Pa	34,994	34,994
$K_{1000\,°C}$	constant	min^{-1}	0.0324	0.0485
$K_{800\,°C}$	constant	min^{-1}	0.0287	0.0345
$k_{1000\,°C}$	constant	$\frac{g}{cm^2 \cdot min}$	3.42×10^{-6}	1.49×10^{-6}
$k_{800\,°C}$	constant	$\frac{g}{cm^2 \cdot min}$	3.02×10^{-6}	1.06×10^{-6}
k^0	pseudofrequency factor	$\frac{g}{cm^2 \cdot min \cdot Pa}$	1.87×10^{-10}	2.65×10^{-10}
E_a	activation energy	J/mole	6.90×10^3	1.93×10^4

can be obtained; $k_{1000°C}$ and $k_{800°C}$ are calculated from Eq. [28]. If we substitute $k_{1000°C}$, $k_{800°C}$, T, and p_{Cl_2} into Eq. [31], E_a and k^O can be calculated.

The results of calculations are summarized in Table V.

V. SOLID PARTICLE MORPHOLOGIES

Although the photos (Figure 7) were taken by picking up the sample area in a random way and the radii and the shapes of the particles in the photos may not reflect the overall average particle size and the general geometry, we can conclude at least the following.

(1) The particles are nonporous and no ash layer was formed during chlorination with either CO or C as reductant. That is in agreement with the previous assumptions made.
(2) When using carbon as reductant, the surfaces of the particles are not as smooth as those when using CO. However, they are still nonporous. The surface roughness was caused by the nonuniform solid-solid contact between TiO_2 and carbon particles.
(3) Particles are irregular.

VI. CONCLUSIONS

1. The reactivity was highly enhanced by carbon compared to CO. The activation energy with C as reductant is much lower than that with CO.
2. There is a difference between the kinetic data of TiO_2(R) and that of TiO_2(A).
3. Reaction rate is first order with respect to chlorine partial pressure by using either CO or C as reductant.
4. Experimental results and thermodynamic calculations established the existence of an activated C-TiO_2-Cl complex when using C as reductant.

LIST OF SYMBOLS

A	surface area of TiO_2 particle, cm^2
BET	BET surface area of TiO_2 powder, cm^2/g
E_a	activation energy for the reaction, J/mol
K	constant, min^{-1}
k	constant, g/(cm^2·min)
k^o	pseudofrequency factor, g/(cm^2·min·Pa)
k_s	rate constant of surface reaction, mole/(cm^2·min·(Pa)$^{n+1}$)
k_s^o	frequency factor, mole/(cm^2·min·(Pa)$^{n+1}$)
M	mass of TiO_2 particle, g
m	reaction order w.r.t. Cl_2
N_i	moles of species i, mole
n	reaction order w.r.t. CO
P_i	partial pressure of species i, Pa
P_{total}	total pressure in the reaction system, Pa
R_i	particle radius of species i, μm (or cm)
R_s	particle radius from sedimentation particle size analysis, μm
R_e	effective particle radius from BET, cm
r	radius of solid particle at time t, cm
r_o	initial radius of solid particle, cm
$V_{unreacted}$	volume of unreacted core, cm^3
V_{total}	total volume of particle, cm^3
ρ_i	molar density of species i, mole/cm^3
ρ^{mass}	density of species i, g/cm^3
τ	time required for complete conversion, min

REFERENCES

1. A. Landsberg: *Metall. Trans. B*, 1975, vol. 6B, pp. 207-14.
2. A. Landsberg: *Metall. Trans. B*, 1977, vol. 8B, pp. 435-41.
3. Karl A. Smith, Steven C. Riemer, and Iwao Iwasaki: *J. Met.*, 1982, Sept., pp. 59-61.
4. A. Toth, I. Berttoti, and T. Szekely: *Thermochim. Acta.*, 1982, vol. 52, pp. 211-15.
5. Jen-Min Chen and Feg-Wen Chang: *Ind. Eng. Chem. Res.*, 1990, vol. 29, pp. 778-83.
6. L. Freitas and F. Ajersch: *Chem. Eng. Commun.*, 1984, vol. 30, pp. 19-33.
7. Anll K. Mehrotra: *Ind. Eng. Chem. Process Des. Dev.*, 1982, vol. 21 (1), pp. 37-50.
8. M. Djona., E. Allain, and I. Gaballah: *Metall. Mater. Trans. B*, 1995, vol. 26B, pp. 703-10.
9. M. Del, C. Ruiz, and J.B. Rivarola: *The Can. J. Chem. Eng.*, 1994, vol. 72, pp. 289-95.
10. I. Gaballah and E. Allain: *Metall. Mater. Trans. B*, 1995, vol. 26B, pp. 711-18.
11. O.L. Culberson et al.: *U.S. Patent* No. 2,832,668, 1958.
12. Rajesh P. Raval and Sharad G. Dixit: *J. Chem. Tech. Biotechnol.*, 1979, vol. 29, pp. 107-15.

13. K.I. Rhee and H.Y. Sohn: *Metall. Mater. Trans. B*, 1990, vol. 21B, pp. 321-30.
14. Robinson: *European Patent* No. 0,096,241, 1983.
15. Robinson: *U.S. Patent* No. 4,619,815, 1986.
16. I. Barin and W. Schuler: *Metall. Trans. B*, 1980, vol. 11B, pp. 199-207.
17. Wendell E. Dunn, Jr.: *Trans. TMS-AIME*, 1960, vol. 218, pp. 6-12.
18. In-Ju Youn and Kyun Young Park: *Metall. Trans. B*, 1989, vol. 20B, pp. 959-66.
19. L. Zhou and H.Y. Sohn: *AIChE J.*, 1996, vol. 42, pp. 3102-12.
20. Bonnie J. McBride and Sanford Gorden: *NASA Reference Publication 1311*, NASA–Lewis Research Center, Cleveland, OH, 1996.
21. Octave Levenspiel: *Chemical Reaction Engineering*, 2nd ed., Wiley, New York, NY, 1972.
22. Hilmar Rode and Vladimir Hlavacek: *AIChE J.*, 1995, vol. 41, pp. 377-88.
23. J. Szekely, J.W. Evans, and H.Y. Sohn: *Gas-Solid Reactions*, Academic Press, New York, NY, 1976.
24. S.S. Tamhankar and L.K. Doraiswamy: *AIChE J.*, 1979, vol. 25, pp. 561-82.